Astronomy & Astrophysics manuscript no. M31_LOFAR_20191022
October 22, 2019

A LOFAR radio search for Crab-like pulsars in Andromeda

Joeri van Leeuwen[1★,2], Klim Mikhailov[2,1], Evan Keane[3], Thijs Coenen[2,1], Liam Connor[2,1], Jason Hessels[1,2], Vlad Kondratiev[1,4], Daniele Michilli[2,1,5,6], Sotiris Sanidas[7,2], and Ben Stappers[7]

[1] ASTRON, the Netherlands Institute for Radio Astronomy, Postbus 2, 7990 AA, Dwingeloo, The Netherlands
[2] Anton Pannekoek Institute for Astronomy, University of Amsterdam, Science Park 904, 1098 XH Amsterdam, The Netherlands
[3] SKA Organisation, Jodrell Bank Observatory, Lower Withington, Macclesfield, Cheshire SK11 9DL, UK
[4] Astro Space Center of the Lebedev Physical Institute, Profsoyuznaya str. 84/32, Moscow 117997, Russia
[5] Department of Physics, McGill University, 3600 rue University, Montréal, QC H3A 2T8, Canada
[6] McGill Space Institute, McGill University, 3550 rue University, Montréal, QC H3A 2A7, Canada
[7] Jodrell Bank Center for Astrophysics, School of Physics and Astronomy, University of Manchester, Manchester M13 9PL, UK

Received . . . ; accepted . . .

ABSTRACT

We observe bright, short bursts of radio emission from sources over a large range of distances: from the nearby Crab pulsar to remote Fast Radio Bursts (FRBs). FRBs are likely to originate from distant neutron stars, but our knowledge of the radio pulsar population has been limited to the Galaxy and the Magellanic Clouds. In an attempt to increase our understanding of extragalactic pulsar populations, and its giant-pulse emission, we employed the low-frequency radio telescope LOFAR to search Andromeda (M31) for radio bursts emitted by young, Crab-like pulsars. For direct comparison we also present a LOFAR study on the low-frequency giant pulses from the Crab pulsar; their fluence distribution follows a power law with slope 2.89 ± 0.02. A number of candidate signals were detected from M31 but none proved persistent. FRBs are sometimes thought of as Crab-like pulsars with exceedingly bright giant pulses – given our sensitivity, we can rule out that M31 hosts pulsars more than an order of magnitude brighter than the Crab pulsar, assuming their pulse scattering follows that of the known FRBs.

Key words. pulsars: general – pulsars:individual:B0531+21 – giant pulses – Galaxies: individual: M31

1. Introduction

In the 50 years since their discovery, millisecond-duration radio signals have helped map out an ever increasing volume of our Universe. Already in the first pulsar, Hewish et al. (1968) recognized the swept pulse delay as interstellar dispersion commensurate with a distance of ~65 pc. Within 20 years the units grew to kpc; McConnell et al. (1991) detected pulsar J0045−7319 in the Small Magellanic Cloud, at 60 kpc. In the last decade, Fast Radio Bursts (FRBs) have been detected that traveled hundreds of Mpc (cf. FRB121102 at luminosity distance 972 Mpc, Tendulkar et al. 2017) and even Gpc (cf. FRB160102 at ~16 Gpc, Bhandari et al. 2018). Dispersion measure studies using pulsars chart out the densities in our Galaxy, while for FRBs these start to map the Universe.

Yet, a gap remains around the 1 Mpc mark. Targeted observations of our neighboring galaxy M31, at 785±25 kpc (McConnachie et al. 2005), may provide insights into the pulsar and/or FRB populations at those distances. Potential benefits of a search of M31 are its relative proximity; its direction well away from the Galactic plane; and its inclination $>10^\circ$ away from edge-on, suggesting modest dispersion measure (DM) contributions internal to M31 to most lines of sight. Less favorable is that its star formation rate over the last $>10^7$ yrs is only about half that of the Milky Way (Yin et al. 2009).

Further to measuring electron densities, extragalactic pulsar detections could sample the intergalactic magnetic field; reveal the most luminous part of the extragalactic population; and enable pulsar population comparisons between galaxies. These necessarily bright pulsars could also fill in the currently existing ten-orders-of-magnitude luminosity gap between known pulsars and FRBs, about which very little if known. For these reasons nearby galaxies were previously searched for fast transients and pulsars (see Mikhailov & van Leeuwen 2016, and references therein). None were successful; but for M31, Rubio-Herrera et al. (2013) carried out a Westerbork Synthesis Radio Telescope (WSRT) search at 328 MHz, and discovered six bursts at the same DM of 54.7 pc cm^{-3}. To be firmly associated with Andromeda, the source needs a DM that exceeds the sum of the foreground Galactic and intergalactic medium (IGM) DMs. Using an IGM density of n_{IGM}=0.16 m^{-3} (Yao et al. 2017) the intergalactic medium between the Milky Way and M31 would contribute only 0.13 pc cm^{-3}, and so does not significantly influence the total. The Yao et al. (2017) Galactic electron density model predicts the maximum Milky Way contribution in this line of sight to be ~60 pc cm^{-3}. The uncertainties in such models, especially at high Galactic latitudes, can exceed a factor of 2 (Deller et al. 2019). Thus the source may be at the outer edge of the Milky Way, or the outer edge of M31. Following it up was a major motivation for the work presented in this paper.

We here report on this M31 search, using LOFAR (van Haarlem et al. 2013). Especially useful is the LOFAR sensitivity; and the observing frequency of 150 MHz, where the pulsar flux density peaks (Stappers et al. 2011) and giant-pulse spectra show little turn over (Karuppusamy et al. 2012). For such extragalactic LOFAR searches, M31 is the highest ranked candidate listed in van Leeuwen & Stappers (2010). We compare the Andromeda

★ E-mail: leeuwen@astron.nl

single-pulse results against the most powerful Galactic giant-pulse emitter, the Crab pulsar[1].

In Sect. 2 we describe the observations and data analysis; in Sect. 3, the search results and M31 rate calculations. In Sect. 4 we contrast the required M31 pulsar flux density distributions to that of the Crab pulsar. We discuss these results and conclude in Sect. 5 and 6. For all these, further background and detail is available in the corresponding Sections of Ch. 4 of Mikhailov 2018 (henceforth M18).

2. Observations and data analysis

The two observations, carried out in 2011 (for 1 h) and 2014 (for 4 h) used the High Band Antennas (HBAs) of the central LOFAR "superterp". Its high filling factor allows for coherent surveying at the highest possible speed (Stappers et al. 2011; Coenen et al. 2014). The observations are detailed in full in Mikhailov (2018); their main characteristics include the use of a pointing grid of around 100 tied-array beams that covers M31, M32 and M110 (Fig. 1); a central frequency around 150 MHz, and bandwidth of 29 and 78 MHz for the two observations respectively; plus a ∼1 ms sampling time and 12 kHz spectral resolution. Data were beamformed, cleaned from basic radio frequency interference (RFI), processed into 8-bit Stokes-I filterbank data using the standard LOFAR pulsar pipeline (Alexov et al. 2010) and stored in the LOFAR long term archive (LTA[2], Renting & Holties 2011).

Data were next dedispersed over a range of trial DMs, determined using the PRESTO (Ransom 2001) dedispersion plan optimizer. The Galactic DM contribution towards M31 is modeled (Yao et al. 2017) to be ∼60 pc cm^{-3} on average, with a foreground gradient over our beam pattern of about ∼7 pc cm^{-3}, increasing toward lower Galactic latitude. The relatively face-on inclination limits the dispersion caused in M31 itself: DMs of order several hundreds pc cm^{-3} are expected (cf. Sect. 5.2).

The 2011 observations were searched from 0−1000 pc cm^{-3}, in 30,000 trials with increasing spacing of 0.01−0.1 pc cm^{-3}. For our observing setup, the intra-channel dispersion smearing for DM=1000 pc cm^{-3} is about 30 ms (Mikhailov 2018), and for DMs above this the signal to noise of narrow bursts decreases further. Following the discovery of high-DM FRBs, the 2014 data were searched up to 2500 pc cm^{-3}, in 45,000 trials. For limited computing time we retain sensitivity to very bright high-DM events there, caused by uncertainties in the DM contributions of the intergalactic medium and M31 itself, or from background FRBs unrelated to M31 (cf. FRB131104; Ravi et al. 2015). While earlier searches for FRBs with LOFAR have not been successful (Karastergiou et al. 2015; ter Veen et al. 2019, cf.), As FRBs have been detected down to 400 MHz (CHIME/FRB Collaboration et al. 2019), where some are narrow and unscattered even at the bottom of band, a detection at LOFAR frequencies could be possible, and would inform us further on the FRB emission properties.

The 2011 data was initially searched for single-pulse emission on the Hydra cluster in Manchester. Data were transferred there from the LTA over a bandwidth-on-demand 1−10 Gbps network. Search output data was partially inspected.

All 2011 and 2014 data were transferred to the Dutch national supercomputer Cartesius[3]. There, we performed dedispersion, periodicity and single-pulse searches using PRESTO (Ransom 2001), over the course of about 325,000 core-hours of Cartesius compute time[4]. All *periodic* candidates from slow (P > 20 ms) pulsar candidates with PRESTO-reported reduced $\chi^2 > 2$ were inspected by eye. We also inspected all *single-pulse* candidates of pulse width W < 100 ms and signal-to-noise (S/N) over 10σ.

3. Search results

3.1. 2011 Observations

The DM = 54.7 pc cm^{-3} bursts identified in Rubio-Herrera et al. (2013) were recorded in a wide-field WSRT mode called 8gr8. This created 8 tied-array beams, each offset within the grating response of the linear WSRT array. That allows for searches over the full field of view of the primary beams of the 25-m dish. The method could only localize this intermittent source to several bands on the sky, as shown in blue in Fig. 1, and reports the two most likely regions at (RA, Dec) = (00h 46m 29s, +41°26′) and (00h 44m 46s, +41°41′). In our 2011 setup these two locations fall in beams 21 and 68. Many other medium- to high likelihood locations fall in other beams.

In the initial pass through the first 1000 seconds of the data, where RFI is low, on the Hydra cluster in Manchester, an excess of pulses at DM = 54.7 pc cm^{-3} was seen in beam 2, at (RA, Dec) = (00h 44m 09s, +41°17′), close to the most likely positions (Fig. 1). These ∼8 individual pulses appear to confirm the candidate pulsar, with a different telescope at a different frequency. Their individual signal-to-noise ratios are in the range 5−6. No other such events were detected in any other beam. No underlying period could be detected from these 8 pulses.

All data were next blindly searched more fully on the Dutch supercomputer Cartesius. We used the LOTAAS single-pulse search pipeline (Sanidas et al. 2019), which is based on PRESTO, to remove RFI and identify individual pulses up to widths of 100 ms. Periodicity searches were carried out as detailed in Mikhailov (2018). We inspected the single-pulse and periodic output both by eye, and with the LOTAAS single-pulse (Michilli & Hessels 2018; Michilli et al. 2018) and periodic (Lyon et al. 2016) machine-learning classifier.

Using this RFI cleaning and pipeline, none of the eight DM=54.7 pc cm^{-3} bursts from the initial pass were redetected. Two were initially found as ∼400 ms wide, and were not detected above the 5σ treshold of the LOTAAS pipeline, at its maximum search width of 100 ms. The six remaining bursts were not automatically redetected by the single-pulse pipeline (Michilli et al. 2018), nor were they identified in manual processing and waterfall plots. New candidate signals did appear in this low-significance regime, at various DMs, suggesting these are statistical fluctuations caused by slight variations in processing. We ruled out the data conversion of PSRFITS to filterbank format, and a number of RFI and masking schemes, as the cause of these fluctuations.

In the 2011 data, some further noteworthy periodic candidates were identified at DMs and in beams other than the candidate above; but none were seen again in the 2014 observations.

3.2. 2014 Observations

A similar blind search through the 2014 data found no convincing pulsar signals from M31, M32 or M110. A close in-

[1] The comparison additionally fitting given the mythological struggle involving Andromeda and the Sea Monster as told by Ovidius (8).
[2] Project data is public at https://lta.lofar.eu/
[3] https://userinfo.surfsara.nl/systems/cartesius
[4] http://www.nwo.nl/onderzoek-en-resultaten/onderzoeksprojecten/i/98/26598.html

spection of even low-significance single-pulse detections around DM=54.7 pc cm^{-3} could not reconfirm the Rubio-Herrera et al. (2013) candidate.

We derive the LOFAR upper limits following from these non-detections using the radiometer-equation based method described in § 3.2 of Kondratiev et al. (2016) and detailed in Mikhailov (2018). Our sky noise estimate includes the continuum contribution from M31 itself. For the periodicity search (ps) our estimated sensitivity $S_{\rm min,\,ps}$ reached in the full 4 hours, for a S/N = 10σ event, assuming a 10% pulse duty cycle, is 1.3 ± 0.7 mJy.

We derive the single-pulse search flux limit using Eq. 3 from Mikhailov & van Leeuwen (2016). For a short single pulse of width $w = 1$ ms, the minimum detectable flux density $S_{\rm min,\,sps}$ is 15 ± 8 Jy. Our minimum detectable *fluence* for a pulse of width w is thus $F_{\rm min}(w) = 15\sqrt{\frac{w}{1\,{\rm ms}}}$ Jy ms.

4. Comparison of giant pulses from the Crab pulsar to the M31 search

Given this sensitivity, could we detect bright giant pulses (GPs) from young neutron stars in Andromeda? To determine this, we compare against the brightest known specimen, the Crab pulsar. Below we derive its LOFAR fluence distributions, and extrapolate to determine the odds of detecting bright, super-giant pulses (Cordes 2004; Cordes & Wasserman 2016) from M31.

4.1. The Crab pulsar at LOFAR frequencies

Earlier multi-frequency studies of Crab GPs spanned the radio spectrum from 20 MHz with LWA to 15 GHz with Effelsberg (for an overview, see Mikhailov 2018). The 430 MHz Arecibo Crab observations by McLaughlin & Cordes (2003) suggest one GP/hr could be seen out to 1 Mpc. M31 is that close, but is out of Arecibo declination range.

To determine if LOFAR could detect Crab-like GPs from M31, we used it to observe the Crab pulsar[5]. The setup was similar to Sect. 2, but with 21 Core Stations, in "Complex Voltage" mode (Stappers et al. 2011) and coherent dedispersion with `CDMT` (Bassa et al. 2017a).

We flux calibrated the data following Bilous et al. (2016). The contribution from the nebula to the station-beam noise is included through the Haslam et al. (1982) 408 MHz map. Furthermore, as our tied-array beam covers ∼1/4th of the Crab Nebula, we add 1/4th of $S_{\rm Crab} \approx 955\,{\rm Jy}\,\frac{\nu}{1\,{\rm GHz}}^{-0.27}$ (Bietenholz et al. 1997) to the background noise budget.

Using this approach, we determine the peak flux density and fluence of all single pulses in our hour of data. Over a downsampling range of 5−500 ms, we identified 4000 pulses whose pulse-integrated S/N ratios exceeded 5σ (a fluence of ∼250 Jy ms). Figure 2 shows an example of the occurrence of multiple pulses within a 1-second window.

The distribution of GP fluence, between our lower limit of 250 Jy ms, and the brightest detected pulse of 1.1×10^4 Jy ms, versus rate, is shown in Fig. 3. The main feature of a power-law fit to its slope is the index, $\alpha = 2.89 \pm 0.02$. We note this is the fit to the differential energy distribution (as plotted in Fig. 3) not to the cumulative distribution that is equally often reported in the literature. Thus, $\alpha = 2.89 \pm 0.02$ describes the slope of the probability density function $p(F) \propto F^{-\alpha}$ as in Karuppusamy et al. (2012), not for the index we shall here call β, which describes the probability distribution $P(F > F_0) \propto F_0^{-\beta}$ as in Sallmen et al. (1999); the relation between the two is that $\beta = \alpha - 1 = 1.89$.

This measurement falls within the range of determinations of the power-law index α at other frequencies (see Karuppusamy et al. 2012 and Table 4.2 in Mikhailov 2018).

4.2. GPs in M31

Using this fluence distribution and rate, we determine whether we could have detected 1-ms wide Crab-like GPs from M31.

For such a pulsar, our minimum detectable fluence $F_{\rm min} = S\,w = 15$ Jy ms. The faintest possible detectable GP from M31 would have to be $F_{\rm Crab,\,M31} = F_{\rm min} \times (D_{\rm M31}/D_{\rm Crab})^2 \sim 2.3 \times 10^6$ Jy ms if it were as close as the Crab. Extrapolating the 1-hr histogram in Fig. 3 suggests that in the 4 hr observation toward M31 the fluence $F_{\rm Crab,\,4hr}$ of brightest detected pulse would be around $1.1 \times 10^4 \times 4^{1/2.89} = 1.8 \times 10^4$ Jy ms. That is about 100× dimmer than our limiting minimum sensitivity from M31.

Yet, the scattering medium to M31 is much less clumped than to the Crab pulsar, and possibly contains no nebula. This means intrinsically short-duration Crab-like GPs (5 μs in Sallmen et al. 1999) from M31 could possibly invoke little scattering. This is seen over even longer distances in FRBs (cf. Fig. 5 of Cordes et al. 2016). If we assume an average DM for sources in M31 of 150 pc cm^{-3} (cf. Sect. 5.2), this FRB relation suggests a scattering time of ∼ 10^{-5} ms at 1 GHz. If we scale as $\nu^{-3.5}$, the scattering time at LOFAR frequencies is around 10 μs. For such a pulsar to have been detected, its 10-μs GP from M31 would have to exceed that of the Crab by a factor $F_{\rm Crab,\,M31}/F_{\rm Crab,\,4hr} \times \sqrt{0.01\,{\rm ms}/1\,{\rm ms}} = 13$.

Our non-detection thus tells us there are no pulsars in M31 beamed at Earth that follow scattering similar to FRBs, that emit GPs an order of magnitude brighter per unit time than the Crab Pulsar.

5. Discussion

5.1. Neutron-star formation in M31

The total star formation rate (SFR) of M31 has been stable over the last few tens of Myr, at ∼1 $M_\odot\,{\rm yr}^{-1}$ (Williams 2003). That is roughly 2 times lower than the SFR in our Milky Way, of 1.9±0.4 $M_\odot\,{\rm yr}^{-1}$ (Chomiuk & Povich 2011). The SFR is important as it maps linearly to neutron star birth rate (cf. Eq. 6 in Keane & Kramer 2008).

The neutron-star low-mass X-ray binaries (e.g., Stiele et al. 2011; Pastor-Marazuela et al. 2019) and X-ray pulsars (Esposito et al. 2016; Rodríguez Castillo et al. 2018) in M31 are clearly evidence for the presence of neutron stars in Andromeda. Further support is provided by its supernova remnants (SNRs). In our Galaxy, 295 are known (Green 2014). A similar number, 156, is identified in M31 (Lee & Lee 2014). Overall, the radio pulsar population in M31 may be somewhat smaller than our Milky Way, but other neutron-star detections clear suggest active pulsars are present.

5.2. Dispersion measure contributions from M31

The electron content of M31 may contribute significantly to the pulse dispersion, reducing detectability especially for sources lo-

[5] Data publicly available under account at the LTA: https://lta.lofar.eu/Lofar?project=ALL&mode=query_result_page&product=UnspecifiedDataProduct&pipeline_object_id=EE400E4EC5D1358CE043C416A9C36F15

cated on its far side. To investigate the scale of this effect, we modified the Yao et al. (2017) electron-density model[6] for our Galaxy, to describe M31. In our own Galaxy both Earth and pulsars are embedded inside the medium. M31 is observed from outside, and we aim to estimate the dispersion smearing to its mid plane. This integration over the full line of sight means the exact value of the electron density and disk scale height by themselves do not strongly influence the outcome. From the M31 mass and major-axis length, we derive the densities and scale heights. We model the gaseous disk using an electron density that doubles from the center out to a radius of 12 kpc and then falls off with a hyperbolic secant squared $\mathrm{sech}^2(x)$ scale length of 8 kpc (Chemin et al. 2009). This is different from the Milky Way, whose thin and thick disk electron densities was modeled out be constant out to 4 and 15 kpc respectively, and then fall off at 1.2 and 2.5 kpc length scales (Yao et al. 2017).

From our model and the orientation of Andromeda in the sky we determine the dispersion measure over our survey field toward sources in the M31 mid plane (Fig. 4). The Galactic foreground of $\sim$60 pc cm^{-3} covers the entire field. In around 20 % of the field we expect twice that. In 10% the expected DM > 180 pc cm^{-3}. All modeled dispersion measures fall within the search space.The intra-channel smearing for the highest DM (> 180 pc cm^{-3}) region is 5 ms, of order 2 samples in the 2011 data and 10 samples in the 2014 data. That is sufficiently low to suggest the deleterious effects of the M31 dispersion are limited, and not a reason for our non-detections.

5.3. Future LOFAR work

The feasibility of detecting Crab-like pulsars from Andromeda depends on both the rate and luminosity of their giant pulses (Fig. 3). Given this rate, for the telescope sensitivity of our current setup, we can extrapolate to the required wait time for a detectable pulse, 13× stronger than the brightest expected pulse in our 4 h observation (cf. §4.2). If the high flux-density tail of this GP distribution is described by the same overall power law, one would need to wait $4\,\mathrm{h} \times 13^{2.89} = 7 \times 10^4$ h for a burst that is bright enough. These results strongly depend on the yet unknown super-giant pulse population (Cordes 2004).

On the other hand, an campaign that significantly improves the luminosity limits is also challenging. For a future LOFAR campaign that reaches the required 13-fold increase in sensitivity, a factor of 4 could be attained by coherently adding not the current 6, but all 24 LOFAR core stations. An order of magnitude more tied-array beams would have to be searched, but these could be preferentially positioned on the M31 disk to maximize discovery potential in a given total observing time. Given the power-law slope of 2.89, the remaining factor of 3 could be overcome through an observing campaign $3^{2.89}$ times longer than our current 4 hr, i.e., $\sim$100 hr. Such an attempt could invest in more computationally-intensive *semi-coherent* dedispersion to limit intra-channel smearing (see, e.g., `CDMT` code and results, Bassa et al. 2017a,b; Maan et al. 2018). As GPs are intrinsically of ns$-\mu$s duration, reducing the dispersive and sampling effects that dilute this signal into the background increases the search sensitivity.

[6] v1.3.2, `http://119.78.162.254/dmodel/ymw16_v1.3.2.tar.gz`

5.4. Other future surveys and follow up

Given its large angular size – the LOFAR observations were almost 4° across – attempts to more deeply search M31 for transients are only possible with wide-field and/or high-survey-speed instruments.

Apertif, the successor to the system used by Braun et al. (2009) and Rubio-Herrera et al. (2013, cf. §3.1), can encompass M31 in a single pointing at 1.4 GHz, and has a powerful time-domain search backend (Oosterloo et al. 2009; van Leeuwen 2014; Maan & van Leeuwen 2017).

A 6-hr integration on M31 with MeerKAT, in the TRAPUM survey (Stappers & Kramer 2016), could detect periodic sources as dim as 3 μJy. If we follow the approach from Mikhailov & van Leeuwen (2016), and simulate one of our most luminous Galactic pulsars, B1641−45, with pseudo luminosity $L_r \gtrsim 6\,\mathrm{Jy\,kpc}^2$, in M31, it would appear as a 10 μJy periodic source.

In single pulse searches of the kind we focused on in this paper, the Square Kilometre Array Mid can detect Crab-like pulsars from over a Mpc (Keane et al. 2015).

Arguably, though, the telescope most likely to find the first if not most pulsars in M31, is the Five hundred meter Aperture Spherical Telescope (FAST; Smits et al. 2009; Li & Pan 2016). At a sensitivity four times that of MeerKAT (Table 1, Dewdney et al. 2013), and given that similar other sources of interest are outside its declination range, a deep campaign will prove profitable.

Our improved localisation of PSR J0044+4117 allows for follow up with narrow-field instruments. Such more sensitive single dishes may enable the identification of its periodicity and spin down.

6. Conclusions

We obtained some of the deepest pulsar search observations of Andromeda but did not detect any new pulsars. A hint of the Rubio-Herrera et al. (2013) candidate was seen in a 2011 beam that covered the original localization pattern, but not confirmed. We observed the Crab pulsar with the same LOFAR setup. We detected thousands of giant pulses, and measured the power-law index of the pulse-brightness probability density function to be 2.89±0.02. We extrapolate this distribution to the longer observation of, and larger distance to, M31. Any pulsar there that outshines the Crab by an order of magnitude, and whose single pulses are scattered the same way as FRBs, we would have detected. We conclude no such super-Crabs beamed at Earth exist in Andromeda.

Acknowledgements. We thank Marten van Kerkwijk for making available `digitize.py`, and Anya Bilous, Jean-Mathias Grießmeier and Michael Kramer for comments on the manuscript. The research leading to these results has received funding from the European Research Council under the European Union's Seventh Framework Programme (FP/2007-2013) / ERC Grant Agreement n. 617199, and from the Netherlands Research School for Astronomy (NOVA4-ARTS). D.M. is a Banting Fellow. This paper is based on data obtained with the International LOFAR Telescope (ILT) under project code LC0_035. LOFAR (van Haarlem et al. 2013) is the Low Frequency Array designed and constructed by ASTRON. It has observing, data processing, and data storage facilities in several countries, that are owned by various parties (each with their own funding sources), and that are collectively operated by the ILT foundation under a joint scientific policy. The ILT resources have benefitted from the following recent major funding sources: CNRS-INSU, Observatoire de Paris and Université d'Orléans, France; BMBF, MIWF-NRW, MPG, Germany; Science Foundation Ireland (SFI), Department of Business, Enterprise and Innovation (DBEI), Ireland; NWO, The Netherlands; The Science and Technology Facilities Council, UK; Ministry of Science and Higher Education, Poland. This work was carried out on the Dutch national e-infrastructure with the support of SURF Cooperative. Computing time was provided by NWO Physical Sciences (project n. 15310).

References

Alexov, A., Hessels, J., Mol, J. D., Stappers, B., & van Leeuwen, J. 2010, in Astronomical Society of the Pacific Conference Series, Vol. 434, Astronomical Data Analysis Software and Systems XIX, ed. Y. Mizumoto, K.-I. Morita, & M. Ohishi, 193
Bassa, C. G., Pleunis, Z., & Hessels, J. W. T. 2017a, Astronomy and Computing, 18, 40
Bassa, C. G., Pleunis, Z., Hessels, J. W. T., et al. 2017b, ApJL, 846, L20
Bhandari, S., Keane, E. F., Barr, E. D., et al. 2018, MNRAS, 475, 1427
Bietenholz, M. F., Kassim, N., Frail, D. A., et al. 1997, ApJ, 490, 291
Bilous, A. V., Kondratiev, V. I., Kramer, M., et al. 2016, A&A, 591, A134
Braun, R., Thilker, D. A., Walterbos, R. A. M., & Corbelli, E. 2009, ApJ, 695, 937
Chemin, L., Carignan, C., & Foster, T. 2009, ApJ, 705, 1395
CHIME/FRB Collaboration, Amiri, M., Bandura, K., et al. 2019, Nature, 566, 230
Chomiuk, L., & Povich, M. S. 2011, AJ, 142, 197
Coenen, T., van Leeuwen, J., Hessels, J. W. T., et al. 2014, A&A, 570, A60
Cordes, J. M. 2004, in Astronomical Society of the Pacific Conference Series, Vol. 317, Milky Way Surveys: The Structure and Evolution of our Galaxy, ed. D. Clemens, R. Shah, & T. Brainerd, 211
Cordes, J. M., & Wasserman, I. 2016, MNRAS, 457, 232
Cordes, J. M., Wharton, R. S., Spitler, L. G., Chatterjee, S., & Wasserman, I. 2016, ArXiv e-prints
Deller, A. T., Goss, W. M., Brisken, W. F., et al. 2019, ApJ, 875, 100
Dewdney, P. E., Turner, W., Millenaar, R., et al. 2013, http://www.skatelescope.org/wp-content/uploads/2013/03/SKA-TEL-SKO-DD-001-1_BaselineDesign1.pdf
Esposito, P., Israel, G. L., Belfiore, A., et al. 2016, MNRAS, 457, L5
Green, D. A. 2014, Bulletin of the Astronomical Society of India, 42, 47
Haslam, C. G. T., Salter, C. J., Stoffel, H., & Wilson, W. E. 1982, A&AS, 47, 1
Hewish, A., Bell, S. J., Pilkington, J. D. H., Scott, P. F., & Collins, R. A. 1968, Nature, 217, 709
Karastergiou, A., Chennamangalam, J., Armour, W., et al. 2015, MNRAS, 452, 1254
Karuppusamy, R., Stappers, B. W., & Lee, K. J. 2012, A&A, 538, A7
Keane, E., Bhattacharyya, B., Kramer, M., et al. 2015, Advancing Astrophysics with the Square Kilometre Array (AASKA14), 40
Keane, E. F., & Kramer, M. 2008, MNRAS, 391, 2009
Kondratiev, V. I., Verbiest, J. P. W., Hessels, J. W. T., et al. 2016, A&A, 585, A128
Lee, J. H., & Lee, M. G. 2014, ApJ, 786, 130
Li, D., & Pan, Z. 2016, Radio Science, 51, 1060
Lyon, R. J., Stappers, B. W., Cooper, S., Brooke, J. M., & Knowles, J. D. 2016, MNRAS, 459, arXiv:1603.05166 [astro-ph.IM]
Maan, Y., Bassa, C., van Leeuwen, J., Krishnakumar, M. A., & Joshi, B. C. 2018, ApJ, 864, 16
Maan, Y., & van Leeuwen, J. 2017, ArXiv e-prints
McConnachie, A. W., Irwin, M. J., Ferguson, A. M. N., et al. 2005, MNRAS, 356, 979
McConnell, D., McCulloch, P. M., Hamilton, P. A., et al. 1991, MNRAS, 249, 654
McLaughlin, M. A., & Cordes, J. M. 2003, ApJ, 596, 982
Michilli, D., & Hessels, J. W. T. 2018, SpS: Single-pulse Searcher
Michilli, D., Hessels, J. W. T., Lyon, R. J., et al. 2018, MNRAS, 480, 3457
Mikhailov, K. 2018, PhD thesis, University of Amsterdam, Ch. 4, http://hdl.handle.net/11245.1/d3a5406f-eb36-4bb8-a280-54a3eedd0a52
Mikhailov, K., & van Leeuwen, J. 2016, A&A, 593, A21
Oosterloo, T., Verheijen, M. A. W., van Cappellen, W., et al. 2009, in Wide Field Astronomy & Technology for the Square Kilometre Array, 70
Ovidius, P. N. 8, in Metamorphoses, ed. A. Golding (London: W. Seres)
Pastor-Marazuela, I., Webb, N. A., Wojtowicz, D., & van Leeuwen, J. 2019, A&A, *submitted*
Ransom, S. M. 2001, PhD thesis, Harvard University
Ravi, V., Shannon, R. M., & Jameson, A. 2015, ApJ, 799, L5
Renting, G. A., & Holties, H. A. 2011, in Astronomical Society of the Pacific Conference Series, Vol. 442, Astronomical Data Analysis Software and Systems XX, ed. I. N. Evans, A. Accomazzi, D. J. Mink, & A. H. Rots, 49
Rodríguez Castillo, G. A., Israel, G. L., Esposito, P., et al. 2018, ApJ, 861, L26
Rubio-Herrera, E., Stappers, B. W., Hessels, J. W. T., & Braun, R. 2013, MNRAS, 428, 2857
Sallmen, S., Backer, D. C., Hankins, T. H., Moffett, D., & Lundgren, S. 1999, ApJ, 517, 460
Sanidas, S., Cooper, S., Bassa, C. G., et al. 2019, A&A, 626, A104
Smits, R., Lorimer, D. R., Kramer, M., et al. 2009, A&A, 505, 919
Stappers, B., & Kramer, M. 2016, in Proceedings of MeerKAT Science: On the Pathway to the SKA. 25-27 May, 9
Stappers, B. W., Hessels, J. W. T., Alexov, A., et al. 2011, A&A, 530, A80
Stiele, H., Pietsch, W., Haberl, F., et al. 2011, A&A, 534, A55
Tendulkar, S. P., Bassa, C. G., Cordes, J. M., et al. 2017, ApJ, 834, L7
ter Veen, S., Enriquez, J. E., Falcke, H., et al. 2019, A&A, 621, A57
van Haarlem, M. P., Wise, M. W., Gunst, A. W., et al. 2013, A&A, 556, A2
van Leeuwen, J. 2014, in The Third Hot-wiring the Transient Universe Workshop, ed. P. R. Wozniak, M. J. Graham, A. A. Mahabal, & R. Seaman, 79
van Leeuwen, J., & Stappers, B. W. 2010, A&A, 509, A7
Williams, B. F. 2003, AJ, 126, 1312
Yao, J. M., Manchester, R. N., & Wang, N. 2017, ApJ, 835, 29
Yin, J., Hou, J. L., Prantzos, N., et al. 2009, A&A, 505, 497

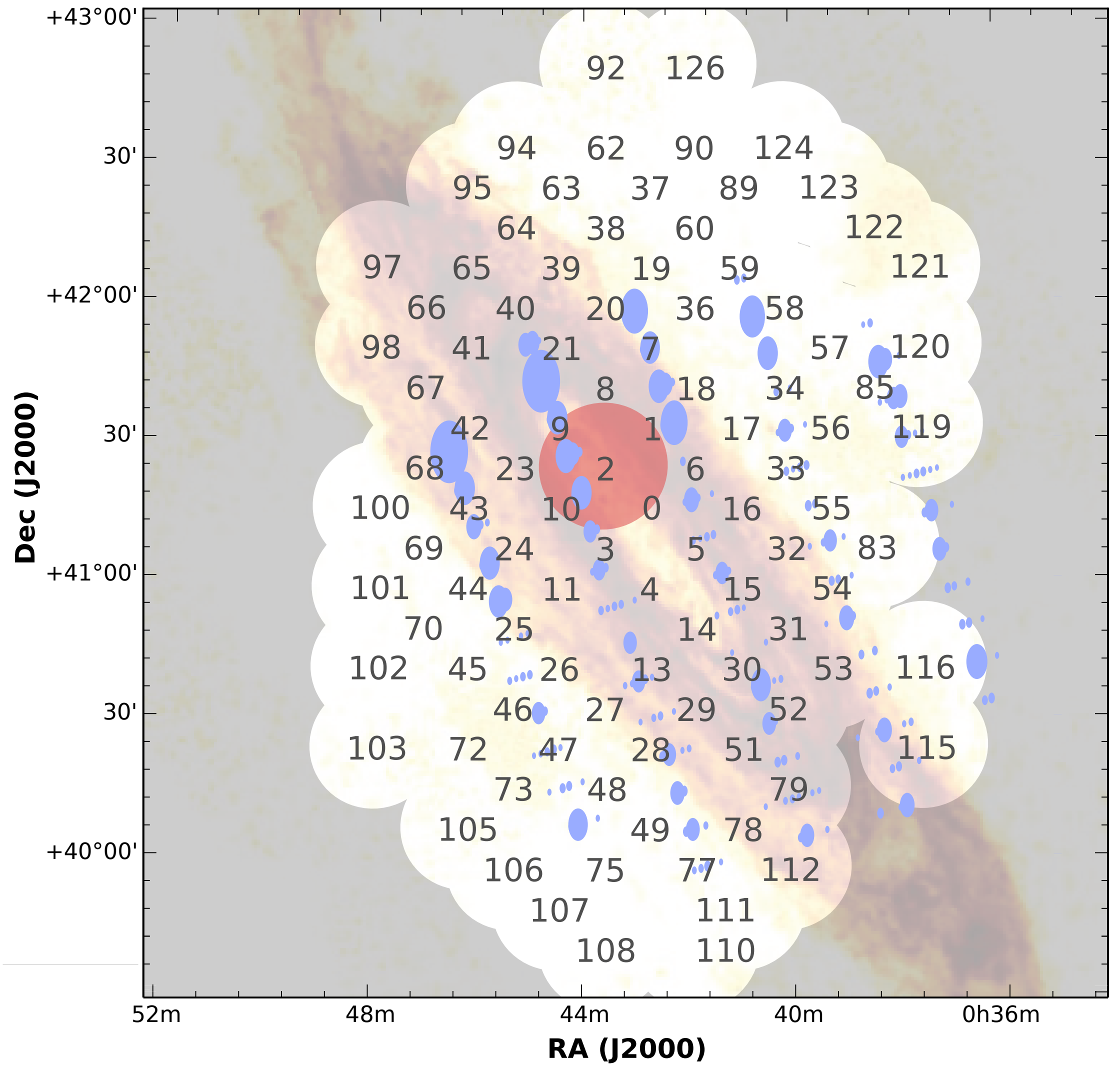

Fig. 1: The union of our 2011 beam pattern with the localization distribution of the DM = 54.7 pc cm^{-3} candidate from Rubio-Herrera et al. (2013) in blue. The overall outline and beam numbers over the 2011 observation are shown; the 25 absent beams failed initial processing. As observations were taken around transit, the beams are close to circular. The size of the blue ellipses indicates the S/N of the DM = 54.7 pc cm^{-3} single-pulse detection in the WSRT subbeam at that location. In red, the LOFAR beam in which most pulses from this candidate were detected. In the background, the H I peak brightness map at 60 arcsec and 6 km s^{-1} resolution, as observed with WSRT (Braun et al. 2009). The 91 tied-array beams pattern from 2014 overlaid on a 10-hr LOFAR imaging observation of M31 is found in Mikhailov (2018).

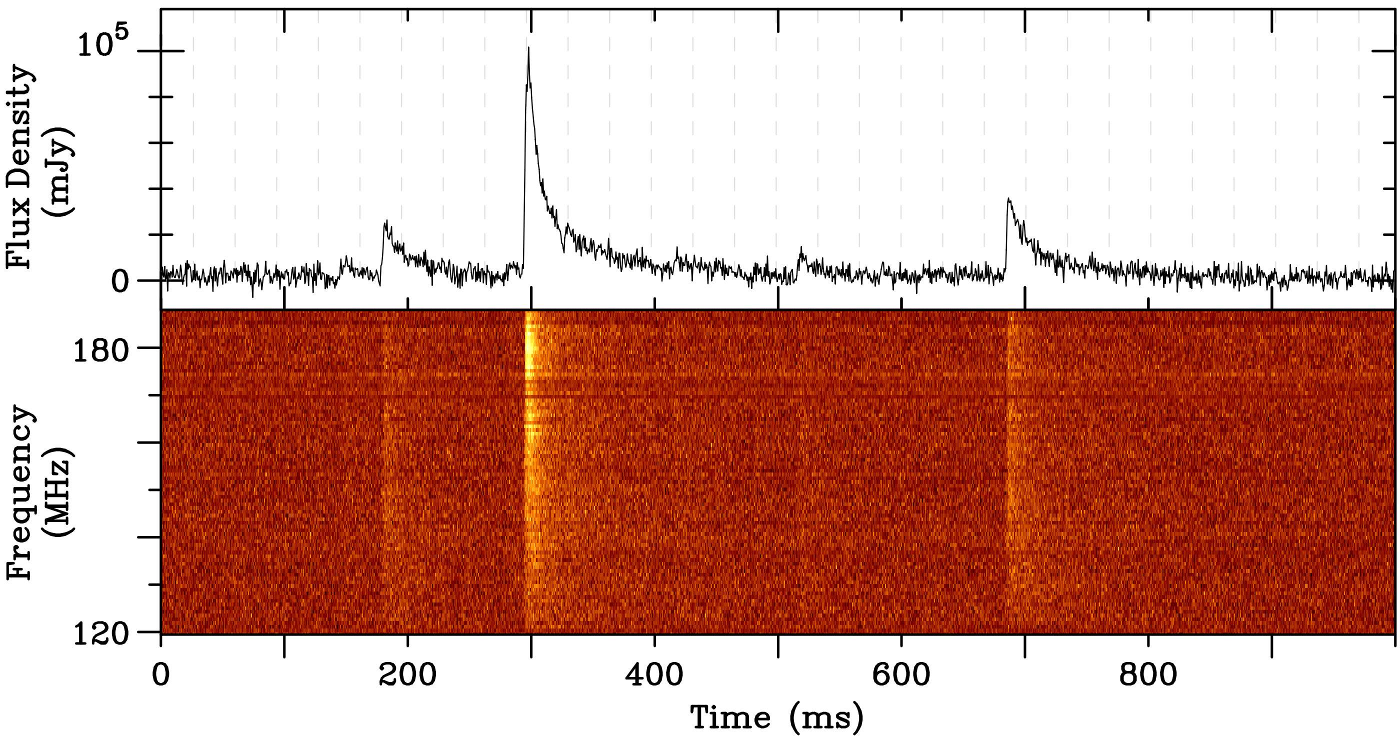

Fig. 2: One second of LOFAR data containing multiple Crab giant pulses. Dashed lines indicate the same phase as the onset of the highest pulse. Giant pulses occur at both main and inter pulse phase.

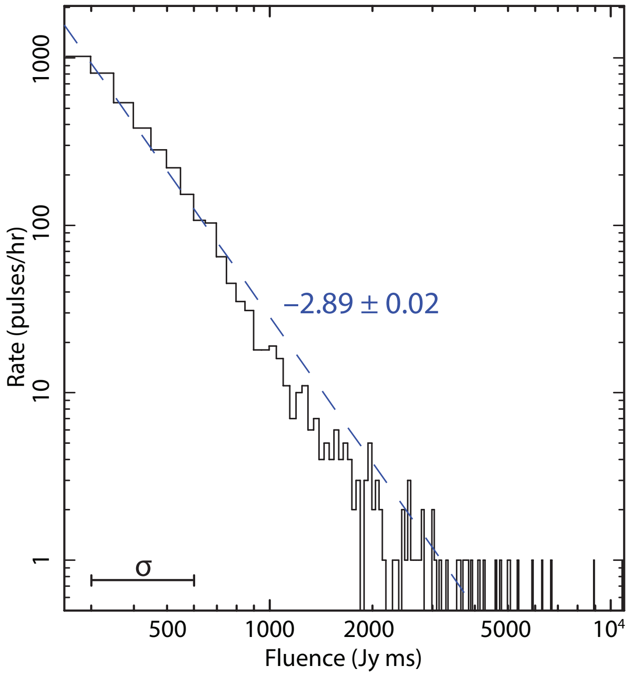

Fig. 3: The Crab fluence distribution as measured in the same setup as the LOFAR M31 search, plus the power-law best fit. The measurement error σ on the fluence values is indicated bottom-left.

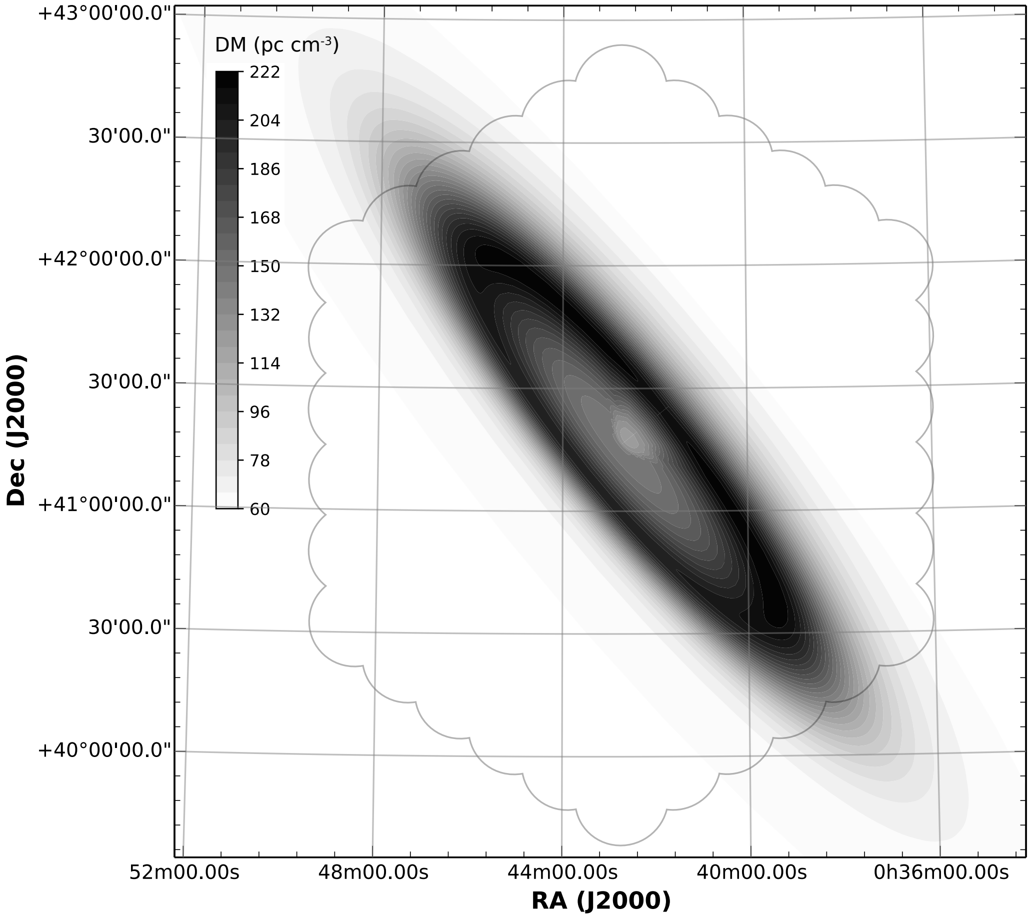

Fig. 4: Expected total dispersion measure for sources in the mid plane of M31. The galactic foreground is seen throughout. The 91 tied-array beam pattern from the 2014 observation is shown in outline.